Microchemical Journal 190 (2023) 108582

Contents lists available at ScienceDirect

Microchemical Journal

journal homepage: www.elsevier.com/locate/microc

Dynamics of diffusion, evaporation, and retention of organic solvents in paints by unilateral NMR and HR-MAS NMR spectroscopy

Valeria Di Tullio [a,b,*], Roberta Pigliapochi [b], Nicholas Zumbulyadis [c], Silvia A. Centeno [b], Jaclyn Catalano [d], Molly Wagner [c], Cecil Dybowski [c]

[a] Institute of Heritage Science (ISPC), CNR, Via Salaria km 29, 300, Montelibretti (RM), Italy
[b] Department of Scientific Research, The Metropolitan Museum of Art, New York, NY, USA
[c] Department of Chemistry and Biochemistry, University of Delaware, Newark, DE, USA
[d] Department of Chemistry and Biochemistry, Montclair State University, Montclair, NJ, USA

ARTICLE INFO

Keywords:
Solvents
Paintings
Linseed oil
Diffusion
NMR
Swelling

ABSTRACT

Transport of organic solvents in polymeric matrices plays a central role in many processes of interest to the coatings industry. Previous studies have focused on individual processes taking place in the solvent-paint system. In the present study, we report results on the molecular dynamics in a solvent/paint system during the entire sequence of absorption, diffusion, swelling, and evaporation processes, obtained non-invasively, *in situ*, and in real time using unilateral NMR relaxometry. The associated chemical structures were investigated using HR-MAS NMR spectroscopy. Four distinct ranges of molecular motion in the solvent/paint film were identified based on proton NMR transverse relaxation time (T_2) data. The fast motion of the freely moving solvent molecules was discriminated from the slower motion of the so-called bound phase of the solvent molecules physically and chemically interacting with the cross-linked polymer network. In addition, two distinct domains of the cross-linked and mobile phases of the polymerized oil were observed, allowing the study of both the dynamics of the swelling-contraction process of the polymer and of the solubilization process. Such non-invasive analyses provide significant information on transport phenomena of the solvent in the paint film, as well as on the effects of various solvents applied to oil paintings.

1. Introduction

The manufacture of coatings is a batch process that involves the mixing of pigments, polymeric binders, and additives dispersed in organic solvents or water as the carrier. Although solvents and additives are mainly used to control the viscosity of the final product, they also indirectly affect many of the properties of the coatings such as drying time, durability, compatibility with other coatings, and emission of volatile organic compounds to the environment [1]. Molecular transport of solvents through swollen networks is a key process that critically determines the performance of such coatings [2,3]. The solvent/paint interactions that determine the ultimate properties of the coatings discussed in this paper, are controlled by processes like diffusion, evaporation, retention, leaching, and swelling [4].

Several studies have focused on the individual processes taking place in the solvent-paint system. The degree of swelling in mock-up paint samples treated with a range of organic solvents was studied by Stolow in 1957 using an instrument based on a parallel plate viscometer to measure changes in thickness, while free films were measured under a microscope [5,6]. Based on the models of Hildebrand [7] and Hansen [8], Teas proposed the first three-dimensional map of solubility [9] in which the solvent/polymer interactions were expressed by three parameters, f_d, f_h, f_p, related to dispersion forces, hydrogen bonds, and dipolar intermolecular forces, respectively. More recently, various experimental techniques have been utilized to characterize the behavior of solvent/paint systems and to study the properties of solvents in polymers. These techniques include differential refractometry, optical microscopy, fluorescence spectroscopy, interferometry, FT-IR spectroscopy, and nuclear magnetic resonance (NMR) spectroscopy [10]. An integrated modeling of the aforementioned processes is challenging because each of them requires a different theoretical and experimental approach.

Our interest in solvent/paint interactions is motivated by the need to understand the effects of treatments undertaken by museum

* Corresponding author.
E-mail address: valeria.ditullio@cnr.it (V. Di Tullio).

https://doi.org/10.1016/j.microc.2023.108582
Received 17 September 2022; Received in revised form 24 February 2023; Accepted 27 February 2023
Available online 2 March 2023

professionals for the conservation of easel paintings. In the conservation of cultural heritage, the removal of aged varnishes is one of the most important treatments performed by conservators. Cleaning paintings is an irreversible process that may cause damage to the surfaces [11–13]. Recently, the solvent treatment has been identified as an important factor that could seriously compromise the conservation of artworks by accelerating degradation processes such as the formation of metal soaps [14,15]. In this context, the details of solvent/paint interactions are important for optimizing the cleaning of painted surfaces and the removal of varnishes.

In the case of easel paintings, the study of solvent/paint interactions is hindered by additional complicating factors. While providing relevant information, Stolow's instrumental method cannot be applied to paintings, as it would be invasive and thus, from a conservation standpoint, unacceptable. Feller's solubility test, [16] based on the Teas diagram, is the easiest method to determine the polarity of the surface of painted objects (expressed by the parameter f_p). Despite it being easy to perform, this solubility test does not give information about swelling, leaching, or retention of solvents. A gravimetric approach involving small fragments collected from a real painting and treated with several organic solvents has been proposed by Masschelein-Kleiner [17]. Because of its invasive nature, this method cannot be applied routinely. More recently portable analytical methods such as Fourier transform laser speckle imaging (FT-LSI) [18], unilateral NMR spectroscopy, and solid phase microextraction (SPME) [19] have been applied to the characterization of solvent effects in artistic paintings and laboratory mock-ups.

NMR spectroscopy [20,21] and unilateral NMR are powerful techniques for studying the chemical-physical properties of polymers and coatings by the analysis of ^{1}H NMR relaxation times T_1 and T_2, proton depth profiles, and self-diffusion coefficients [22,23]. Unilateral NMR has the additional advantage of carrying out these analyses without physical sampling, thereby completely preserving the integrity of the object under investigation [24–29]. Information about the dynamic properties of solvent molecules and binder polymer chains can be inferred from the relaxation of ^{1}H spins [30]. The return of spins to thermal equilibrium in an external magnetic field, following various radiofrequency (rf) pulse sequences, is characterized by two relaxation time constants: the spin–spin (T_2) and the spin–lattice (T_1) relaxation time. The magnitude of each of these parameters depends on the interaction of spins with each other and with the environment. These interactions are modulated by molecular motions.

Because they are non-invasive, unilateral NMR methods have been applied to the characterization of processes in art conservation. Examples include their use to evaluate the stratigraphy of paintings [31,32], the changes in paint thickness after the removal of varnish layers [33], the absorption and diffusion of water into acrylic-based paints [34,35], and the removal of degraded coatings on mural paintings [36]. Other studies have reported the evaluation of T_2 times of paint layers. Fire *et al.* [37] studied the embrittlement of the binder due to the action of solvents in a painting by analyzing the average T_2 of the polymerized oil before and after treatment. Prati *et al.* [19] recently used ^{1}H NMR depth profiles and the distribution of transverse T_2 relaxation times to characterize the physicochemical properties of paint layers in contact with eco-friendly gels by observing the changes in polymer mobility.

Recently, our group reported the distribution of T_2 and the self-diffusion coefficients of water to calculate the open porosity of an oil paint layer, showing that water molecules in such systems are in a restricted-diffusion regime [38]. However little information is available about the nature of the various dynamic environments of organic solvents imbibed in paintings.

In this paper, we present results on the dynamics of solvents of varying polarity in paint films made from linseed oil and basic lead white. The observed ^{1}H T_2 data, obtained by unilateral NMR, is strongly non-exponential, indicating dynamic heterogeneity. We show that analysis of the T_2 data reveals several distinct dynamic states for the solvent and the binder polymer chains. We illustrate the ability to differentiate between solvent and polymer signals by the use of deuterated solvents, an approach used in unilateral NMR studies for the first time in this paper. Finally, we combine the results of unilateral NMR with proton high resolution magic angle spinning NMR (^{1}H HR-MAS NMR) to gain an understanding of the solvent-binder interactions at the molecular level.

2. Materials and methods

2.1. Preparation of the paint films and solvent exposure

Model paint films 500 μm thick were prepared following the protocol described in reference [38], where more details about the procedure can be found. Briefly, lead white (Sigma-Aldrich, $2PbCO_3.Pb(OH)_2$) and pure linseed oil (Kremer Inc.) were mixed in a 5:1 w/w pigment-to-oil ratio and the mixture was applied on a canvas substrate using a manual film applicator. The samples were cured for nine months at room temperature, and subsequently subjected to accelerated aging in an oven at 65 °C for one week.

Each film was exposed to one of the following solvents: acetone, deuterated acetone (acetone-d_6), ethanol, and mineral spirits (a mixture of aliphatic, or alicyclic C_7 to C_{12} hydrocarbons). The paint samples were exposed to solvents by imbibing six sheets of filter paper in the solvent for 10 min, leading to an overall 2 g of solvent absorbed. The six imbibed sheets were then stacked over the paint film, which was placed over a glass slide for support. The whole glass/paint film/filter sheets assembly was then wrapped in plastic foil to reduce evaporation. To evaluate the absorption process, the imbibed sheets were left on the paint film for a total of 160 min, during which time the unilateral NMR analysis was conducted. After this time, to evaluate the evaporation process, the plastic foil and the filter sheets were removed, while the paint film was left on NMR probe for the rest of the analyses.

After completion of the NMR measurements, one paint film was further re-dried by heating it at 65° for 8 h in an oven. To evaluate the effects of consecutive applications of the solvent, the sample was then exposed to ethanol once again for a second cycle of absorption, by following the same procedure previously described.

2.2. Unilateral NMR

^{1}H depth profiles and spin–spin relaxation times (T_{2eff}) were measured at 0.36 T (proton Larmor frequency of 18 MHz) with an NMR-MOUSE® (MObile Universal Surface Explorer), consisting of an electronic unit manufactured by Bruker Biospin interfaced to a single-sided ACT sensor (RWTH Aachen University, Aachen, Germany) [27]. By unilateral NMR, a CPMG echo-decay envelope was measured under a strong inhomogeneous magnetic field, as a consequence the transverse relaxation time is shorter than the one acquired under a homogeneous magnetic field and is usually called the *effective* T_{2eff}. Relaxation times were measured from the damping of echoes in a CPMG pulse sequence consisting of 4096 echoes, with an echo time of 41 μs, a recycle time of 1 sec, 2048 scans. Each CPMG sequence was acquired for a total time of approximately 27 min. The following measurement started after approximately three minutes, to space the data by 30 min. Before exposing each paint film to the solvent, a ^{1}H depth profile was acquired, and a T_2 relaxation time was measured at the center of the film thickness. Once the filter sheets imbibed with the solvent were placed on top of the paint film, a ^{1}H depth profile was acquired, and T_{2eff} was measured at the center of the film – thickness-wise – every 30 min for 160 min (segment I, absorption phase). The response to a CPMG sequence was acquired 200 μm from the paint surface with a resolution of 100 μm. Then the imbibed sheets were removed and the procedure was repeated, by acquiring the ^{1}H depth profile first, followed by a T_{2eff} measurement at the center of the paint-film for 340 min (segment II, evaporation phase). The whole process lasted for 500 min.

2.3. HR-MAS NMR spectroscopy

High resolution magic angle spinning (HR-MAS) proton spectra were acquired on a Bruker Avance II-600 NMR spectrometer (Bruker Biospin, Karlsruhe, Germany). The spectrometer was equipped with a triple-resonance 4-mm probehead, which included a ^{2}H lock channel and a magnetic field gradient coil whose axis was aligned along the spinning axis. All measurements were carried out at 27 °C. 60 μg of the lead carbonate linseed oil sample was held with acetone-d_6 (f_d = 47), methanol-d_4 (f_d = 30) and cyclohexane-d_{12} (f_d = 96) in a rotor with a volume of 12 μL, using a spin rate of 5 kHz to increase the spectral resolution. A diffusion filter was applied using the stimulated-echo experiment with bipolar gradient pulses and a longitudinal eddy current delay ("ledbpgp1d" from the Bruker pulse-program library), at a magic angle spinning speed of 5 kHz. Each 1D-diffusion spectrum was acquired from 1024 acquisitions, a spectral width of 6009.6 Hz, and a data size of 32 K points. The T_2-filter was implemented with a CPMG ("cpmgpr1d" from the Bruker pulse-program library) sequence having a suitable echo time of 2 ms (192 loops, rotor-synchronized interpulse delay of 0.4 ms) and a recycle delay of 4 s, with a magic angle spinning speed of 5 kHz.

2.4. Data processing

In unilateral NMR, the analysis of NMR signals is carried out without a Fourier transform of the time-domain data, allowing the study of the time evolution of the nuclear magnetization. This approach permits the study of domains with different dynamics.

Because the transverse relaxation time, T_2 depends on the molecular motions, protons in solids and cross-linked macromolecules relax rapidly, whereas protons in small molecules, in liquid and low-viscosity phases relax more slowly. To obtain physico-chemical information of the molecular system and to characterize the different dynamic domains of proton nuclei, appropriate techniques of data processing must be applied. It is well-known that in a liquid the decays of the longitudinal and transverse magnetizations of proton nuclei are described by a single exponential, usually with $T_1 \cong T_2$ on the order of seconds. In the case of highly viscous materials, non-crystalline polymers, and liquids in porous materials, the proton nuclei exhibit multi-exponential decays with values of T_1 and T_2 distributed over a large time scale (μs-sec) [39]. Often magnetization decay data are analyzed by fitting them to discrete exponentials, however in heterogeneous systems relaxation time constants should not be reported without analyzing the data for a distribution of relaxation times.

Many studies have proposed different methods based on the inverse Laplace transform (ILT) to convert the relaxation decay into a continuous distribution of relaxation components, however all of them are intrinsically affected by numerical problems and the reported solutions may not be unique [40,41]. Nevertheless, the decomposition of the T_2 decay into a sum of exponential decays remains a common practice used in phenomenological models of complex systems, where the more complex the molecular dynamics, the more exponential terms are required [42]. Supposing an NMR signal $S(t_k)$ measured at echo times t_k with (k = 1,2, …, n), the decay of the transverse magnetization can be described as the sum of up to N exponential decays as shown in:

$$S(t_k) = \sum_{i=1}^{N} A_i e^{-\frac{t_k}{T_{2i}}} \quad (1)$$

A mono or bi-exponential analysis of materials with different T_2 time constants is a relatively accurate method as opposed to more complex systems with a number of exponentials N ≥ 3, where the T_2 relaxation becomes a non-trivial problem. Thus, in our study the T_2-distribution was used as a reference method to map out the number of distinct T_2 components and measure the range of T_2 values. Based on multi-exponential functions, our model was focused on searching for the minimum number of exponential components able to fit the decays with the highest R^2 and the best residuals distribution (see Figure S1 in Supplementary information). All calculations concerning the T_2 relaxation were performed in Sigmaplot (Systal Software Inc) apart from the distribution of T_2 which was carried out in Matlab 2015a (Mathworks, Natick, Ma, USA) using the UPEN algorithm [43].

A duplicate measurement was performed to estimate the reproducibility of the data set. Due to the lack of temperature control and the fact that time-consuming acquisition of data show high error, the average relative standard deviation in T_{2cr} and T_{2mp} was ~20%, whereas in T_{2bs} and T_{2fs} was ~10%. The average relative standard deviation in the weight fraction W_i for all components was found to be ~10%.

3. Results and discussion

3.1. Transverse relaxation times and the solvent-paint polymer motional regime

The interaction between a solvent and a paint film is a complex process that depends on the diffusion of the solvent in the polymeric network as well as the solubility and swelling properties of the polymer. In a dynamic, multi-phase system, the interpretation of the observed multicomponent transverse relaxation rate requires the determination of the number of distinct proton dynamic states and their fraction of the total proton population as well as a molecular-level model for their relative mobility.

Fig. 1 shows 2D-contour plots of the T_2-distributions obtained as a function of the solvent application time in three linseed oil-lead white paint films (PbLO) treated with ethanol, acetone, or mineral spirits (each single distribution is reported in the Supplementary information file, figure S2).

An analysis of the T_2-distribution indicates a complex multimodal distribution of relaxation times, consistent with the presence of four main distinct dynamic states, each with its own characteristic median transverse relaxation time.

The relaxation time T_2 ranges of the four distinct dynamic states in Fig. 1, are:

1. [0.1–0.8] ms slow-motion domain (characterized by long correlation times and short T_2).
2. [1–8] ms first intermediate-motion domain.
3. [10–50] ms second intermediate-motion domain.
4. [70–120] ms fast-motion domain (short correlation times, T_2 long).

In general, the decay rate of the magnetization is affected by the molecular dynamics (restricted chain motions, rotation, translation), changes in molecular weight, order, packing, and temperature. A unique description of the molecular motions contributing to the transverse relaxation in a multi-phase system is not straightforward. Standard Bloembergen–Purcell–Pound (BPP) theory describes the relaxation constants in terms of molecular dynamics assuming that the autocorrelation function of the microscopic fluctuations causing the relaxation can be described by a single correlation time, τ_c [44]. The theory agrees well with experiments in homogeneous systems. Disordered heterogeneous systems require a more complex computational treatment [44]. In paints, besides the chemical composition, the T_2 is strongly affected by the polymer chain mobility, order and packing. An appropriate analysis of T_2 data can reveal information about the macro-scale dynamics of the system. However, in the present case, because of the complexity of the system and the processes involved, such as evaporation, absorption, swelling, solubilization, and diffusion, it is not possible to unequivocally assign each individual T_2 mode shown in the 2D-maps of Fig. 1. Furthermore, the T_2-distribution is sensitive to noise and is susceptible to artifacts. Nevertheless, it is possible to propose a basic molecular-level model based on the minimum number of dynamic states resolved using a multi-exponential function.

To describe the dynamic heterogeneity of the system we propose a multi-phase model associating each of the four dynamic states (identi-

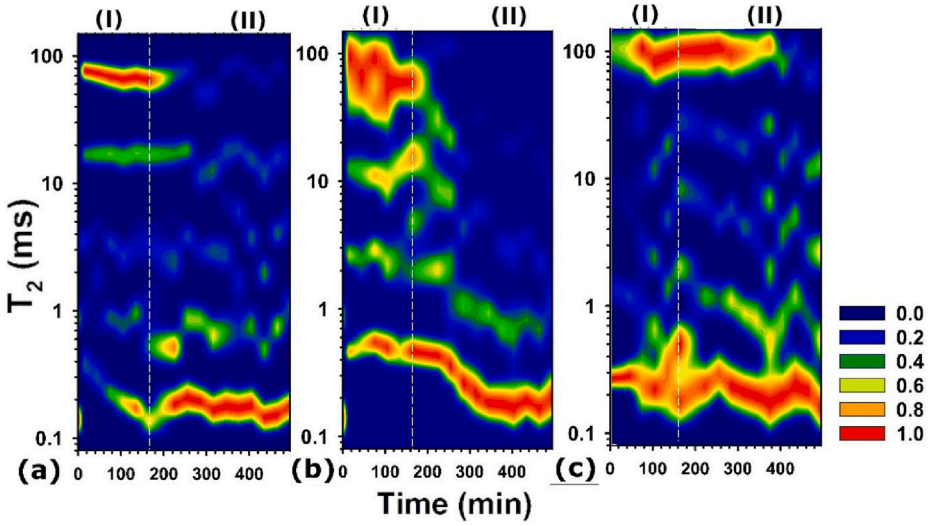

Fig. 1. T_2 distributions as a function of time in a linseed oil-lead white paint film (PbLO) after solvent application. a) Acetone; b) ethanol; and c) mineral spirits. The white dashed lines divide the absorption segment (I) from 0 to 160 min from the evaporation segment (II) from 160 to 500 min. The color gradient encodes the population density normalized on the maximum value of each distribution.

fied by the four distinct components of T_2 linked to the dynamic ranges listed above) with possible structures at the molecular level. The overall relaxation behavior f(t) is then given by:

$$f(t) = A_{cr}{}^{*}e^{\left(\frac{t}{T_{2cr}}\right)} + A_{mp}{}^{*}e^{\left(\frac{t}{T_{2mp}}\right)} + A_{bs}{}^{*}e^{\left(\frac{t}{T_{2bs}}\right)} + A_{fs}{}^{*}e^{\left(\frac{t}{T_{2fs}}\right)} \quad (2)$$

Where:

- T_{2cr} is the relaxation time T_2 of protons in aliphatic chains of the "cross-linked" oil phase.
- T_{2mp} is the relaxation time T_2 of protons in the "mobile oil" phase.
- T_{2bs} is the relaxation time T_2 of protons in the "bound" phase of the solvent.
- T_{2fs} is the relaxation time T_2 of protons in the "freely moving" phase of the solvent.
- A_{cr}, A_{mp}, A_{bs}, and A_{fs} are the respective fractions of proton density contributing to each of the four dynamic states T_2s.

Unlike NMR spectroscopy, unilateral NMR does not provide chemical information. The following hypothetical model for the molecular level structures giving rise to the four proton dynamic states is proposed. The T_2 values of the four phases based on our model are reported in Fig. 2. The cross-linked oil phase, T_{2cr}, arises from protons on the relatively rigid framework of the polymeric network. However, not all protons in linseed oil are part of this network. The protons in saturated acyl chains, polymer segments plasticized by the solvent and polymer regions of low cross-link density are more mobile than the protons in the fully cured cross-linked polymer and their dynamic state contributes to the "mobile oil" phase, T_{2mp}. The presence of these species is a function of the degree of polymerization, and therefore time dependent, and varies for each time segment within the experimental sequence. These two components of T_2 are also found in the dry oil paint-film (t = 0) where the T_2-decay can be modelled by a bi-exponential function [30].

The overall relaxation behavior of the solvent-paint system is also determined by protons belonging to the solvent that was applied to the surface of the paint. Our model is consistent with two dynamic states for the protons assigned to the solvent: one with a short relaxation time, T_{2bs}, related to a "bound" solvent phase and another with a long transverse relaxation time, T_{2fs}, related to the "freely moving" solvent. We assume that the bound phase of the solvent, T_{2bs} arises *mostly* from solvent molecules whose mobility is restricted by interactions at the polymer/solvent interface or confinement within the polymer. However, protons from polymer chain ends and small oligomers solvated by the solvent may also contribute to the signal.

Finally, we assume that the more mobile fraction of the solvent, T_{2fs}, is dominated by the free translational motion of solvent molecules through the polymeric network. The fraction of this dynamic state strongly depends on the amount of solvent absorbed by the paint, the path length of the unrestricted diffusion, the length of time the solvent was applied, and the environmental conditions such as temperature and relative humidity. However, free triglycerides not yet polymerized and leached-out chain-scission products could also contribute to this fraction. It is also important to note that the apparent value of the T_{2fs} component might be the most affected by the strong magnetic field gradient of the unilateral NMR apparatus and the impact of diffusion.

During the absorption of the solvent (segment I), T_{2cr} showed a slight increase in the paint sample treated with ethanol, whereas it was mostly unchanged in acetone, and shortened in mineral spirits (Fig. 2a). After the removal of the solvent (segment II), T_{2cr} linearly decreases in ethanol and acetone, reaching a constant value at longer evaporation times. The T_{2cr} in minerals spirits remained mostly unchanged for the whole process. The weight fraction of the cross-linked oil in mineral spirits showed the same evolution. On the contrary, the weight fractions of the cross-linked oil component in ethanol and acetone decrease first (segment I) and then, at longer evaporation times (segment II), increase, showing a similar trend without reaching the values found in the dry paint (Fig. 2c).

After the first 15 min of solvent application, in the presence of ethanol and acetone, our results show a fast reduction of the proton mobility in the mobile oil phases T_{2mp}, (Fig. 2b). The reduced mobility of the protons in the oil mobile phase is most likely due to the leaching out of small oligomers that act as plasticizers. We hypothesize that these small molecules at the equilibrium swelling migrate across the mesh of the polymer into the solution, thus their protons motion contribute to the fractions of the bound and free solvent phases.

After this first fast reduction, the values of T_{2mp} do not change as a function of time in segment I. At this time, a quasi-stationary state is reached where the transport of the molecules from the polymer surface into the solution prevents an increase of the swollen layer and a further absorption of the solvent [10]. Both T_{2cr} and T_{2mp} may be affected by the swelling of the polymer, by the solvent and the stretching-contraction of polymer chains [45,46]. As reported by Stolow, the swelling equilibrium state in an oil paint layer is reached in a few minutes (5–10 min) [6]. However, the time-to-equilibrium swelling greatly depends on the solvent and the depth at which the film is probed. Considering the inter-diffusion coefficients for acetone and ethanol reported in reference [47]

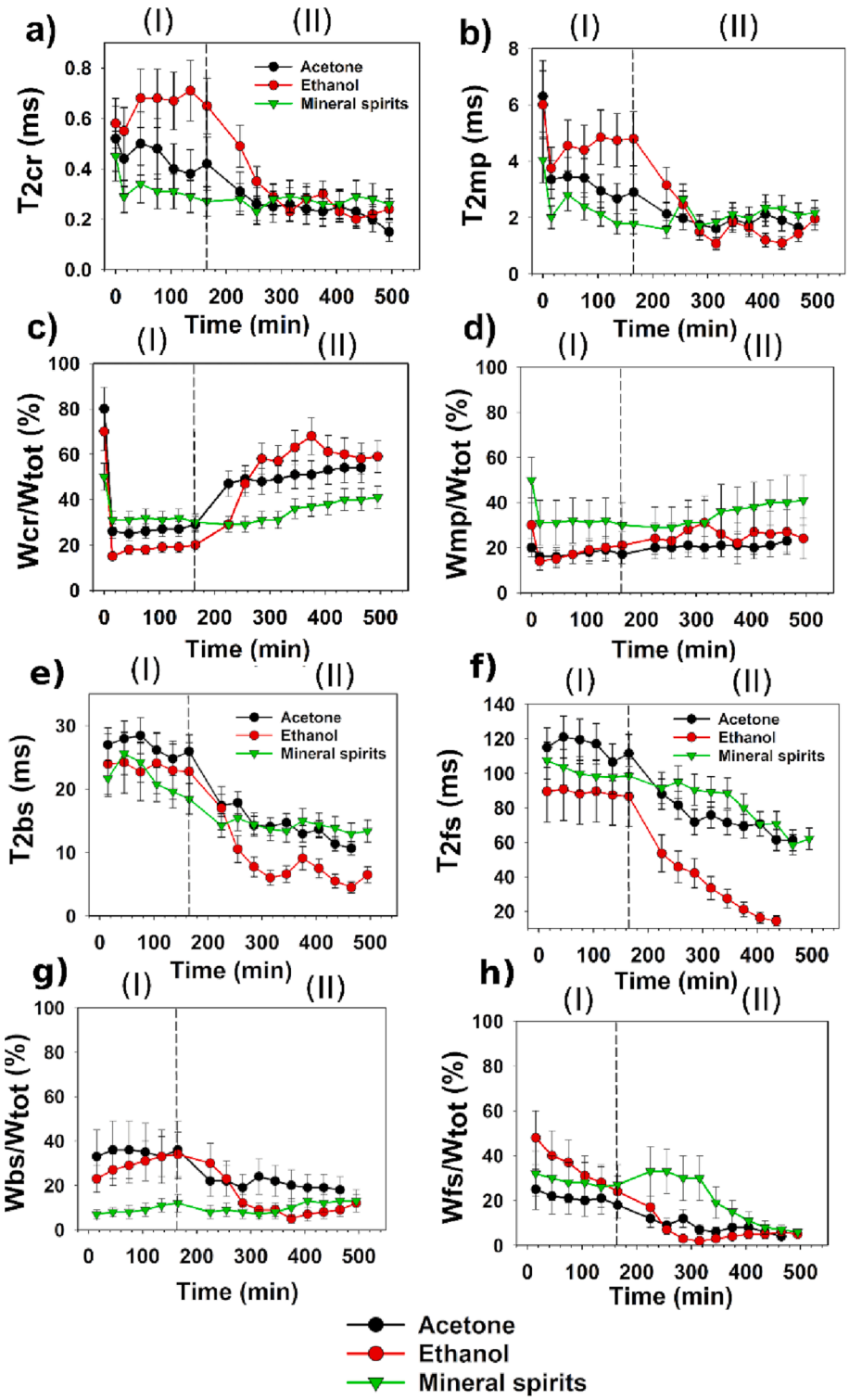

Fig. 2. Transverse relaxation times T_2 (ms) versus time elapsed from the initial application of solvent. a) Cross-linked phase of the PbLO; b) mobile domain of the PbLO; c) and d) normalized relative weight of each T_2 component in % for cross-linked and mobile domain of PbLO, respectively. Transverse relaxation times T_2 (ms) of e) bound solvent domain; f) solvent free-moving domain; g) normalized relative weight of the bound solvent domain; h) normalized relative weight of the free-moving solvent domain. W_i is the weight of each T_2 component and is expressed as $\frac{A_{i\perp}}{A_{t0}}$* 100 were $A_{t0} = \sum_{i=1}^{N} A_i$ (N = 4). Black dashed lines divide the absorption segment (I) from 0 to 160 min and the evaporation segment (II) from 160 to 500 min.

and the depth probed by unilateral NMR, we estimate that the equilibrium swelling is reached after 3 min for acetone and 55 min for ethanol. To our knowledge, for mineral spirits in lead-oil paints, no interdiffusion coefficient has been published, however considering the interdiffusion coefficient of cyclohexane we estimated that the equilibrium swelling might be reached in approximately 200 min. It is important to note that these interdiffusion coefficients were obtained in a non-porous model paint system whereas in a porous oil paint film, as those used in our experiments [38], the equilibrium swelling could be reached faster.

From this reference data, we hypothesize that, in segment I, in the time-scale of our experiment, a gel-liquid layer in equilibrium with the swollen polymer is formed in which the solvent is partially bound and free-moving as showed by the T_{2bs} and T_{2fs} (Fig. 2e and f). At this time, the weight fractions of protons in the bound phase W_{bs} in acetone and ethanol were found to be greater than the one in mineral spirits. Acetone and ethanol diffuse faster than mineral spirits and they have a higher capability of extraction of small polar oligomers [48]. During segment II, this equilibrium is broken because the solvent absorbed by the paint

evaporates causing the contraction of the polymer network (shrinking), thus the values of T_2 decrease in all motion domains (Fig. 2e and 2f).

To understand the various interactions during the evaporation process (segment II) better, we compared the T_2 values acquired in acetone and deuterated acetone (Fig. 3). By using deuterated solvents, the signals from the solvent protons can be suppressed leaving only the signals from the oil phases. Unlike the hydroxyl proton in ethanol, acetone-d_6 has no exchangeable protons under the conditions of our experiments.

As expected, the T_{2cr} and T_{2mp} values show similar trends regardless of solvent deuteration, consistent with our assignment of these two dynamic states to cross-linked and mobile oil phases respectively (Fig. 3a and b). On the other hand, a different trend is observed in the bound and free-moving solvent phases T_{2fs} and T_{2bs} (Fig. 3c and d). In acetone-d_6, the proton mobility is faster (longer T_{2fs}) than that observed in acetone (Fig. 3c). After 100 min of evaporation, the proton mobility decreases and no contribution of the longest T_{2fs} is observed.

On the other hand, the T_{2bs} values for acetone and acetone-d_6 show a

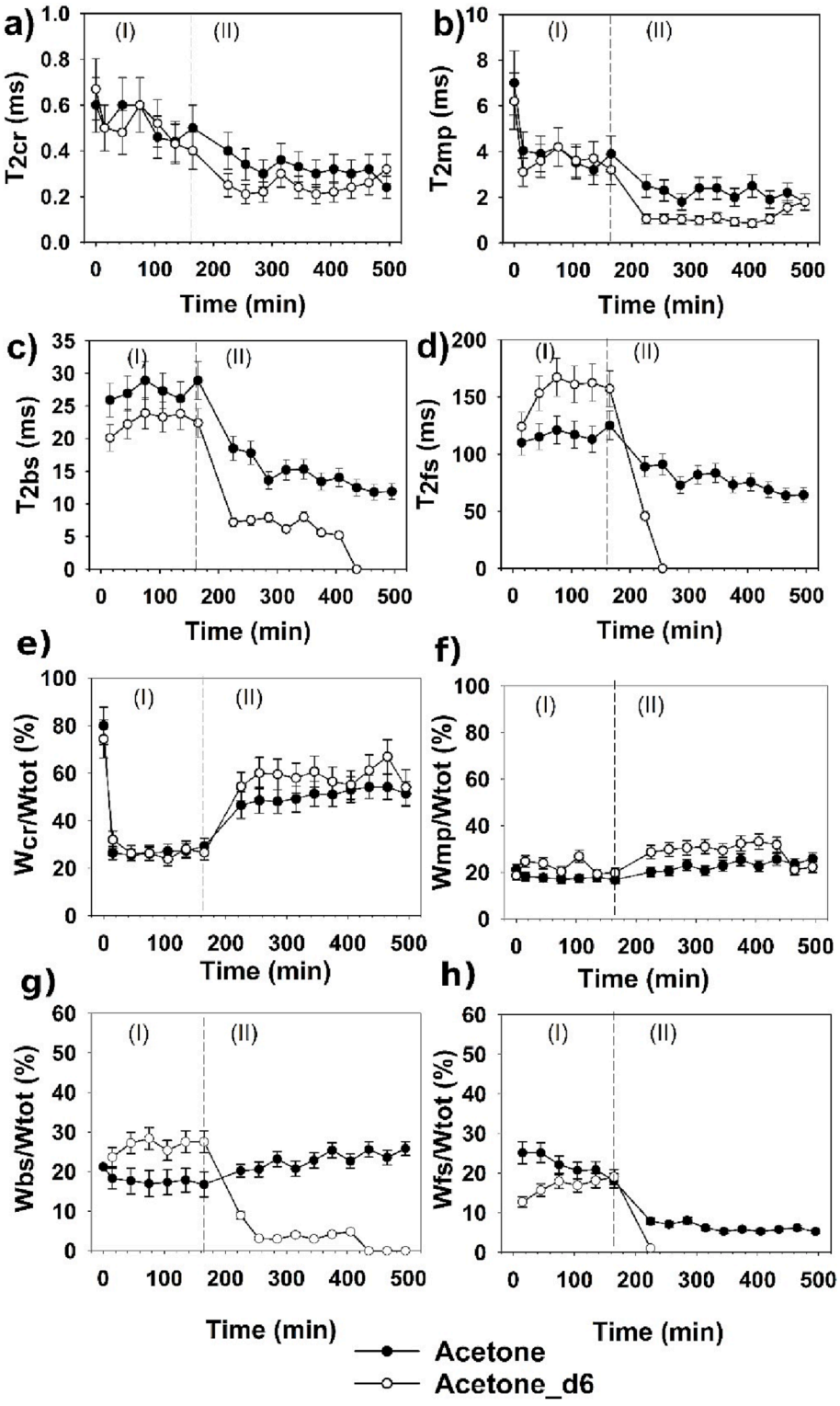

Fig. 3. Transverse relaxation times T_2(ms) vs time elapsed since the application of acetone and acetone-d_6. Mobility domains: a) cross-linked oil protons; b) mobile oil protons; c) bound solvent; and d) free-moving solvent. e) and f) normalized relative weight of each T_2 component in % for the cross-linked and mobile domains of PbLO, respectively; g) normalized relative weight of the bound solvent domain; h) normalized relative weight of the free-moving solvent domain. Black dotted lines divide the absorption phase (I) from 0 to 160 min; and the evaporation phase (II) from 160 to 500 min.

similar time dependence (Fig. 3c) but a different time dependence in the weight fraction of the bound phase, W_{bs} (Fig. 3g). These results indicate that some moieties of the cross-linked oil phase are plasticized by the bound phase of the solvent along with the polar small oligomers that are solvated. This effect is completely masked by the solvent protons when using non-deuterated acetone. In fact, the weight fraction of the bound phase W_{bs}, in deuterated acetone show a fast decrease during the evaporation phase (segment II), indicating that the contribution of protons of solvated small oligomers and polymer moieties persist until the gel-liquid layer is in equilibrium with the swollen polymer (Fig. 3h). During segment II, due to solvent evaporation, the diffusive motion of these molecules is quickly hindered, as they might possibly precipitate or form larger micellar structures.

Little information is available about the effect of the oil polymer–solvent interface on molecular motion. The interaction between some moieties of the polymer with the solvent molecules may also delay the evaporation of the solvent causing its retention in the paint, as we observed at long evaporation time where a residual proton mobility of the acetone is still observed (Fig. 3e).

3.2. ^{1}H HR-MAS NMR spectroscopy to chemically analyze the solvent-paint polymer system

To characterize the liquid-gel layer, we acquired ^{1}H HR-MAS NMR spectra of the polymerized oil and lead white paint swollen in acetone-d_6, methanol-d_4 and cyclohexane-d_{12}. HR-MAS NMR spectroscopy is a powerful tool for the characterization of soft matter and multiphase-systems [49,50]. HR-MAS produces high resolution spectra without the extraction processes required in liquid-state NMR spectroscopy, preserving the polymer network structure suitable for the swollen state examination. The ^{1}H HR-MAS spectra obtained in the swollen paint samples with deuterated acetone, methanol, and cyclohexane are reported in Fig. 4a, b, and c, respectively.

The ^{1}H HR-MAS NMR spectra (Fig. 4 a, b and c) in all solvents show the most intense signals in the spectral range from 0.85 to 1.2 ppm due to protons of the aliphatic chains. Detailed resonance assignments are given in Table 1.

In all spectra, the overlap between sharp and broader resonance bands due to protons with different mobilities at the liquid-polymer interface is observed. It is well known that, in the absence of inhomogeneous broadening, the line width is inversely proportional to the effective relaxation rate. The ^{1}H HR-MAS spectrum shows better resolution because the local mobility is increased by using deuterated solvents and by the reduced contribution of dipolar interactions and anisotropic shift interactions. Differences in magnetic susceptibility are reduced by magic angle spinning. However, in polymers the spinning rate is not sufficient to suppress the effects of strong ^{1}H–^{1}H dipolar coupling, and some macromolecules moieties may show larger bands overlapping those which spread in the swollen polymer network. By combining diffusion (PFG-SE) and T_2-filter (CPMG) sequences, it is possible to carry out spectral editing, and fast, slow, and static moieties can be successfully separated. Under the use of a diffusion filter, ^{1}H HR-MAS spectra may show resonances due to macromolecular moieties that are not diffusing but have a residual mobility mostly due to the protons in unsaturated aliphatic chains (Figs. 4 a1, b1, and c1). By using a CPMG T_2-filter, the PbLO paint spectra show only the sharper signals mostly due to the diffusing molecules of the esterified and free fatty acid resonances. Interestingly, in acetone and ethanol, the glycerol proton resonance at 4.4 ppm is still observable, while the resonances at 5.3–5.5 ppm from unsaturated vinyl protons are completely truncated (Figs. 4 a2, b2, c2).

These results are consistent with the observations reported by Kehlet *et al.* for ultra-fast MAS solid-state NMR spectroscopy measurements on Zn-containing paint samples. These authors suggest that their results indicate the presence of a mobile fraction due to triglycerides (TG) that are partially cross-linked. In addition, the signal is also attributable to an extractable fraction composed of free fatty acids (FFA), di-glycerides, and mono-glycerides [51]. Further research is needed to extract more quantitative information, and to calculate the correlation times and the self-diffusion coefficients of the species involved in the liquid-polymer interface.

3.3. Swelling degree calculated by NMR T_2 decay

As previously reported, transverse relaxation times allow a determination of the number of dynamically distinct populations in the solvent-paint system. Another important piece of information that can be obtained by fitting T_2-decays is the swelling capacity of the polymer during solvent absorption and evaporation. The swelling capacity is defined as the change in the dimensions of the polymer and can be calculated by different methods [49]. One of the simplest methods is to calculate the ratio between the volume fraction or weight of the polymer before and after the absorption of a solvent. As the solvent volume fraction increases in the polymer meshes, one expects to observe an increase in the proton density. By extrapolating the proton density, A_t, to zero time, following eq.3, one can obtain a value directly correlated to the free volume of the solvent. In this study, we calculated the swelling degree (SD) as a percentage of the ratio between the total proton density in the dry polymer (A_{t0d}) and the total proton density in the swollen polymer (A_{t0s}) as a function of time, using the following equation:

$$SD_{NMR(\%)}=(A_{t0s}-A_{t0d})/A_{t0s} * 100 \quad (3)$$

During the evaporation phase (segment I), the swelling degree remains mostly unchanged. In the case of acetone, a reduction is observed, probably due to the evaporation of the solvent. However, due to the significant error associated with the limited resolution of unilateral NMR, the time-consuming acquisition, and the lack of temperature control during the absorption phase, the change may be smaller than appears in Fig. 5.

During the evaporation phase (segment II), the paints treated with mineral spirits show a slower drying speed compared to the paints treated with ethanol and acetone; at long evaporation times, the drying of the polymer network in ethanol and acetone reaches a constant value whereas in mineral spirits it continues to decrease. This result is not surprising, as shown previously in Fig. 2h, the weight fraction of free-solvent in mineral spirits, W_{fs}, decreases more slowly than in ethanol and acetone. For all solvents, the degree of swelling after 500 min of evaporation does not return to the initial value (Fig. 5).

To check the sensitivity of the SD_{NMR}, we applied ethanol II cycle to the same sample after it was dried in an oven for two days at 45 °C. Interestingly, the sample showed the same kinetics of swelling-drying but had a smaller SD value, which is not surprising since the extraction of plasticizers and a stiffening of the paint may take place after the first solvent application.

4. General discussion and conclusions

In addition to correlating the transverse relaxation times of oil paints during the absorption and evaporation phases, the T_2-based model allows one to discuss how these processes differ depending on the type of solvent.

During the absorption phase, the diffusivity of acetone in paint is greater than that observed for mineral spirits and ethanol, both in the bound- and free-moving phases of the solvent (Fig. 2e-h). It is well known that the diffusivity of acetone in linseed oil paints is greater than that of ethanol and mineral spirits [4].

During absorption, the weight fractions of the bound phase of solvents are greater for acetone and ethanol than for mineral spirits (Fig. 2g). In accordance with the solubility parameters [7,8,52], acetone and ethanol have higher contributions of polar and hydrogen-bond forces than mineral spirits and in oil paints are able to interact with

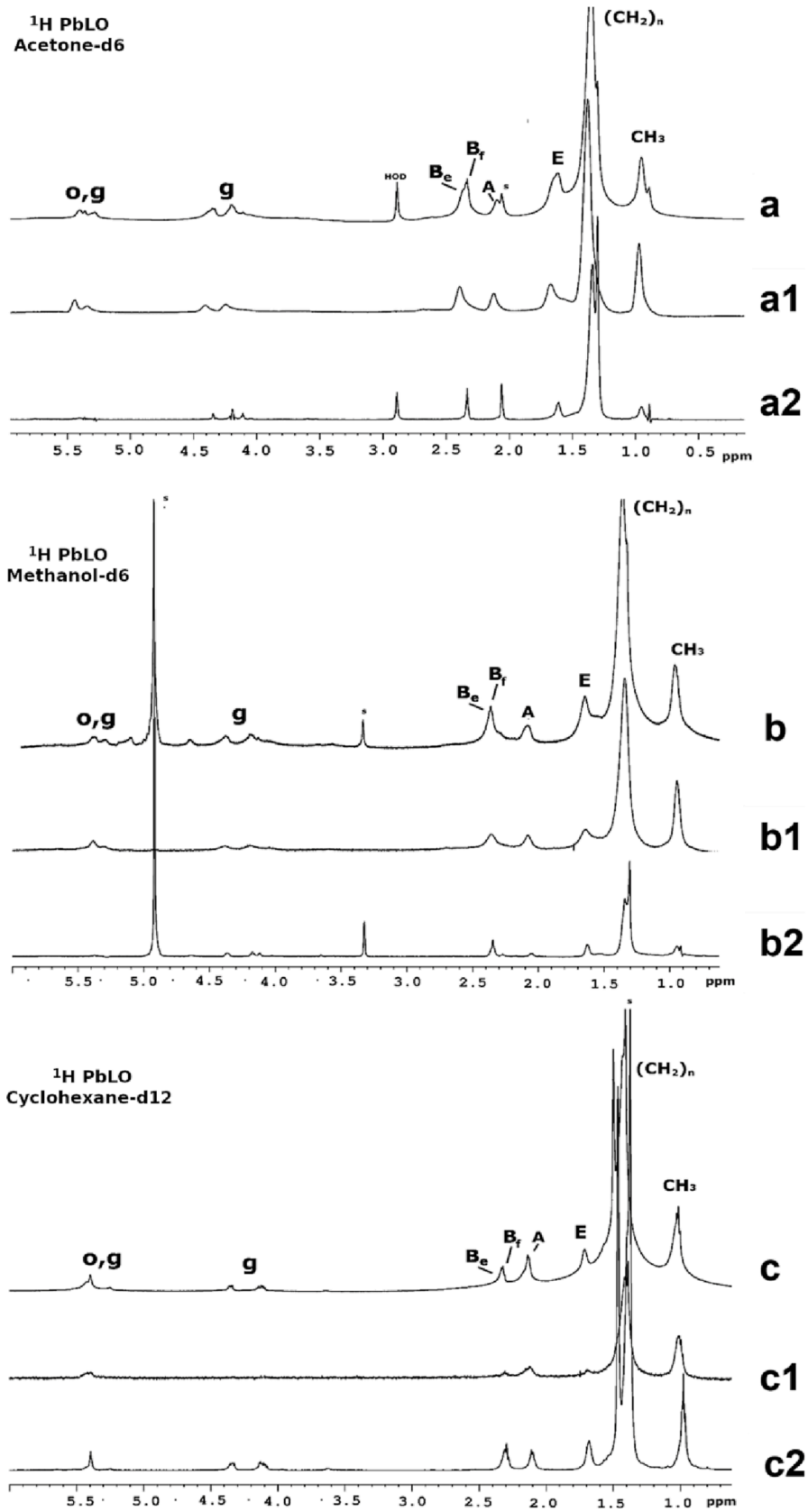

Fig. 4. ^{1}H HR-MAS NMR spectra of linseed oil and lead white paint in a) acetone-d_6; b) methanol_d4; and c) cyclohexane-d_{12}. ^{1}H HR-MAS diffusion filter for the paint samples in a1) acetone; b1) methanol; and c1) cyclohexane. ^{1}H HR-MAS NMR spectra T_2-filter (TE 2 ms) for the paint samples a2) acetone; b2) methanol; and c2) cyclohexane. The labelling of the assignments is summarized in Table 1.

Table 1
Labeling of the assignments in Fig. 4.

Peak	Assignment	
E	CH_2 –CH_2 – COOH	CH_2 second next to carbonyl groups in all FA and diacids
A	CH_2-CH = CH	Allylic protons
Bf	CH_2 –COOH	Methylene groups of FFA and diacids
Be	CH2 –COOR	Methylene group of esterified FA
g	CH–OCOR	Glycerol moiety
o	CH = CH	CH Double bounds
s		Solvent peak

polar groups in small molecules such as –COOH of carboxylic acids and aldehydes arising from hydrolysis and autoxidation of the oil paint. They also interact with hydrogen-bonding acceptors like C = O groups [46,52].

In ethanol, the polymerized oil maintains a higher flexibility during the absorption phase, as demonstrated by the cycle of contraction and stretching due to proton mobility. On the contrary, mineral spirits reduces the paint mobility in both the cross-linked and mobile phases, as compared to ethanol and acetone. Mineral spirits show poor capability to extract small molecules. For example, the weight fraction of its bound phase (W_{bs}) is small in comparison to ethanol and acetone for both absorption and evaporation. Minerals spirits are characterized by a high value of f_d, compared to acetone and ethanol. Clearly, a low value of polarity might increase the probability of interaction between the solvent molecules and the fatty acid chains of the cross-linked triglycerides. As previously reported, the possible interactions between the solvent molecules and some moieties of polymer chains might also affect the dynamics of solvent transport, as well as the equilibrium state at the gel-liquid layer. In fact, ^{1}H HRMAS spectra show better resolution for samples solvated in acetone or cyclohexane (whose f_d value is close to that of mineral spirits) than in ethanol.

During evaporation, the decrease in paint mobility in ethanol is observed after a few minutes, whereas in acetone the paint mobility requires more time for a noticeable effect. At longer evaporation times, the mobility of the oil remains limited in all solvents, indicating that, at the end of oil drying process, all solvents have induced a stiffness in the oil paint film. These results are in accordance with results previously reported [4].

Ethanol was retained by the paint for a shorter period of time than acetone and mineral spirits. In fact, the bound phase of acetone and the free-moving phases of mineral spirits remain in the paint for a longer time than does ethanol (Fig. 2e-h). The degree of swelling of the paint film in mineral spirits shows a slow reduction after 300 min of evaporation. The solvent with the highest retention in the paint is mineral spirits, its solvent bound phase persisting in the paint the longest. Ethanol shows the fastest rate of drying (Fig. 5), in contrast to mineral spirits that shows a very slow decrease of the SD as function of time.

In conclusion, this multi-T_2 component model describes significant qualitative information about the diffusion, evaporation, and retention of solvents in paint layers. The solvent transport through paint layers can be studied by observing the different effects on the mobility of protons in the polymerized oil, as well as by comparing the behavior of different types of solvents. Measurements by unilateral NMR can be applied *in situ*, in a non-invasive manner, on artworks to study the effect of organic solvents in aged and degraded oil paints and to determine their influence in the activation of degradation phenomena.

CRediT authorship contribution statement

Valeria Di Tullio: Writing – original draft, Methodology, Conceptualization, Formal analysis, Investigation, Visualization, Writing – review & editing. **Roberta Pigliapochi:** Investigation, Validation, Conceptualization, Writing – review & editing. **Nicholas Zumbulyadis:** Writing – original draft, Conceptualization, Funding acquisition, Writing – review & editing. **Silvia A. Centeno:** Conceptualization, Funding acquisition, Supervision, Writing - review & editing. **Jaclyn Catalano:** Conceptualization, Writing – review & editing. **Molly Wagner:** Conceptualization, Writing – review & editing. **Cecil Dybowski:** Conceptualization, Funding acquisition, Supervision, Writing – review

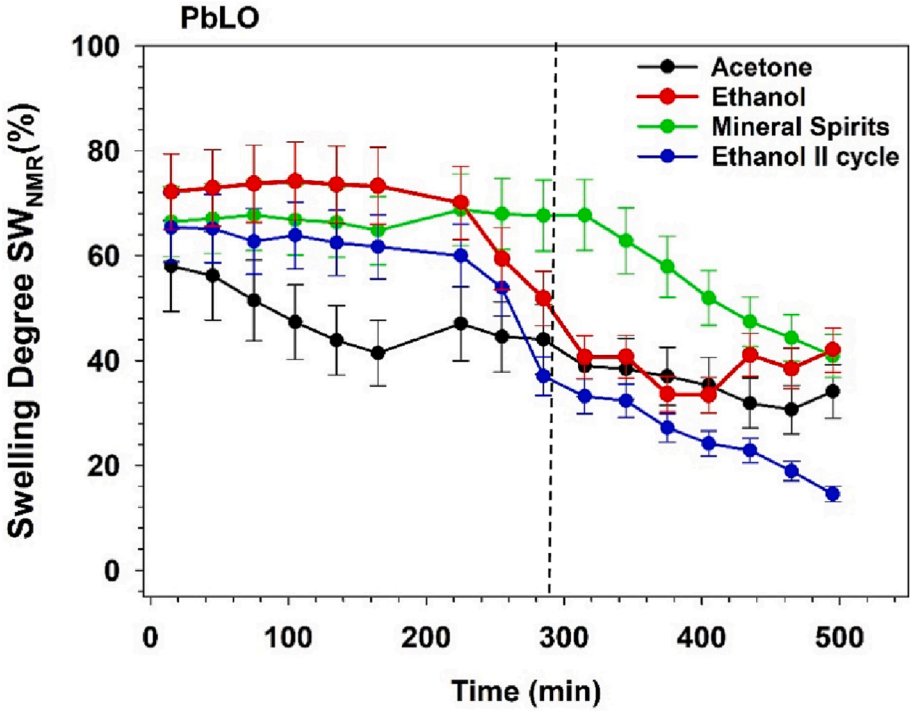

Fig. 5. Swelling degree calculated using equation 3. Black dashed lines divide the absorption segment (I) from 0 to 160 min and the evaporation segment (II) from 160 to 500 min. The relative standard deviation was found to be 15%.

& editing.

Declaration of Competing Interest

The authors declare that they have no known competing financial interests or personal relationships that could have appeared to influence the work reported in this paper.

Data availability

Data will be made available on request.

Acknowledgements

This work was supported by the US National Science Foundation under Grants DMR-1608594 and DMR-1608366 to The Metropolitan Museum of Art and the University of Delaware. We are indebted to Eleonora Del Federico and Cindie Kehlet for sharing the NMR-MOUSE® at the Pratt Institute in New York.

Appendix A. Supplementary data

Supplementary data to this article can be found online at https://doi.org/10.1016/j.microc.2023.108582.

References

[1] A.R. Marrion, The Chemistry and Physics of Coatings, Royal Society of Chemistry (2004), https://doi.org/10.1039/9781847558206.
[2] L. Masaro, X.X. Zhu, Physical Models of Diffusion for Polymer Solutions, Gels, and Solids, Prog. Polym. Sci. 24 (1999) 731–775.
[3] S. Seiffert, J. Sprakel, Physical chemistry of supramolecular polymer networks, Chem. Soc. Rev. 41 (2012) 909–930.
[4] L. Baij, J. Hermans, B. Ormsby, P. Noble, P. Iedema, K. Keune, A review of solvent action on oil paint, Her. Sci. 8 (2020) 43.
[5] N. Stolow, Action of solvents on dried linseed oil films, Nature. 179 (4559) (1957) 579–580.
[6] N. Stolow, A modified apparatus for measuring the swelling of polymer films in solvents, J. Sci. Instrum. 31 (11) (1954) 416–420.
[7] J.H. Hildebrand, R.L. Scott, The solubility of nonelectrolytes, 3rd edn., Dover Publications, Inc., American Chemical Society, New York, 1964.
[8] Hansen, C. M. *Hansen solubility parameters*, London: CRC Press; 2007. DOI: 10.1201/9781420006834.
[9] J.P. Teas, Graphic analysis of resin solubilities, J. Paint. Technol. 40 (516) (1968) 19–25.
[10] B.A. Miller-Chou, J.L. Koenig, A review of polymer dissolution, Prog. Polym. Sci. 28 (2003) 1223–1270.
[11] K. Kahrim, A. Daveri, P. Rocchi, G. de Cesare, L. Cartechini, C. Miliani, B. G. Brunetti, A. Sgamellotti, The application of in situ mid-FTIR fibre-optic reflectance spectroscopy and GC–MS analysis to monitor and evaluate painting cleaning, Spectrochim. Acta A Mol. Biomol. Spectrosc. 74 (5) (2009) 1182–1188.
[12] A. Phenix, K. Sutherland, The cleaning of paintings: effects of organic solvents on oil paint films, Stud Conserv. 46 (sup1) (2001) 47–60, https://doi.org/10.1179/sic.2001.46.Supplement-1.47.
[13] M.F. Mecklenburg, A.E. Charola, R.J. Koestler, *New insights into the cleaning of paintings*, Proceedings from the cleaning 2010 international conference, Universidad Politécnica de Valencia and Museum Conservation Institute, Smithsonian Contributions to Museum Conservation 3 (3) (2013) 1–243, https://doi.org/10.5479/si.19492359.3.1.
[14] L. Baij, A. Astefanei, J. Hermans, F. Brinkhuis, H. Groenewegen, L. Chassouant, S. Johansson, G. Corthals, C. Tokarski, P. Iedema, K. Keune, Solvent-mediated extraction of fatty acids in bilayer oil paint models: a comparative analysis of solvent application methods, Herit Sci. 7 (1) (2019) 31.
[15] Tauber, G.; Smelt, S:; Noble, P.; Kirsch, K.; Siejek, A.; Keune, K.; van Keulen, H.; Smulders-De Jong, S.; Erdman, R.; Evolon, C. R. *Its use from a scientific and practical conservation perspective,* AIC Paint Spec Group Postprints, **2018**, 31, 45–50.
[16] R.L. Feller, N. Stolow, E.H. Jones, On picture varnishes and their solvents, The Press of Case Western Reserve University, Cleveland and London, 1985.
[17] L. Masschelein Kleiner, Les solvants, Institut Royal du Patrimoine Artistique, Bruxelles, 1991.
[18] L. Baij, J. Buijs, J.J. Hermans, L. Raven, P. Iedema, K. Keune, J. Sprakel, Quantifying solvent action in oil paint using portable laser speckle imaging, Sci. Rep. 10 (2010) 1, https://doi.org/10.1038/s41598-020-67115-1.
[19] S. Prati, G. Sciutto, F. Volpi, C. Rehorn, R. Vurro, B. Blümich, L. Mazzocchetti, L. Giorgini, C. Samorì, P. Galletti, E. Tagliavini, R. Mazzeo, Cleaning oil paintings: NMR relaxometry and SPME to evaluate the effects of green solvents and innovative green gels, New J. Chem. 43 (2019) 8229–8238.
[20] N. Bloembergen, E.M. Purcell, R.V. Pound, Relaxation Effects in Nuclear Magnetic Resonance Absorption, Phys. Rev. 73 (1948) 679.
[21] P.T. Callaghan, Translational Dynamics and Magnetic Resonance: Principles of Pulsed Gradient Spin Echo NMR, OUP Oxford, 2011.
[22] Doughty, P.J. and McDonald, P.J. (2005). Hardware and Methods. In NMR Imaging in Chemical Engineering (eds S. Stapf and S.-I. Han). https://doi.org/10.1002/3527607560.ch2c.
[23] A. Szczygiel, NMR of paints, ink, and coatings, in: V. Ramesh (Ed.), Nuclear magnetic resonance 45, 142–143 Cambridge University Press, RSC, Cambridge, 2016.
[24] V. Di Tullio, G. Cocca, R. Avolio, G. Gentile, N. Proietti, P. Ragni, M.E. Errico, Unilateral NMR investigation of multifunctional treatments on stones based on colloidal inorganic and organic nanoparticles, Magn. Reson. Chem 53 (1) (2015) 64–77.
[25] V. Di Tullio, N. Proietti, New Insights to Characterize Paint Varnishes and to Study Water in Paintings by Nuclear Magnetic Resonance Spectroscopy (NMR), Magnetochemistry 6 (2) (2020) 21.
[26] B. Blümich, J. Anders, When the MOUSE leaves the house, Magn. Reson. 2 (2021) 149–160, https://doi.org/10.5194/mr-2-149-2021.
[27] C. Rehorn, B. Blümich, Cultural Heritage Studies with Mobile NMR, Angew. Chem. Int. Ed. 57 (2018) 7304.
[28] V. Di Tullio, D. Capitani, N. Proietti, Unilateral NMR to study water diffusion and absorption in stone-hydrogel systems, Micropor. Mesopor. Mat. 269 (2018) 180–185.
[29] F. Casanova, J. Perlo, B. Blümich, Single-Sided NMR, Springer-Verlag, Berlin Heidelberg, 2011.
[30] B. Blümich, Aging of polymeric materials by stray-field NMR relaxometry with NMR-MOUSE, *Concepts Magn*, Reason. Part A. 47A (2019) e21464.
[31] L. Brizi, V. Bortolotti, G. Marmotti, M. Camaiti, Identification of complex structures of paintings on canvas by NMR: Correlation between NMR profile and stratigraphy, Magn. Reson. Chem. 58 (9) (2020) 889–901, https://doi.org/10.1002/mrc.5054.
[32] F. Busse, C. Rehorn, M. Küppers, N. Ruiz, H. Stege, B. Blümich, NMR relaxometry of oil paint binders, Magn. Reason. Chem. 58 (2020) 830–839.
[33] P. Moretti, L. Cartechini, C. Miliani, Single-sided NMR: a non-invasive diagnostic tool for monitoring swelling effects in paint films subjected to solvent cleaning, Anal. Bioanal. Chem. 412 (5) (2020) 1063–1075, https://doi.org/10.1007/s00216-019-02331-x.
[34] L.V. Angelova, B. Ormsby, E. Richardson, Diffusion of water from a range of conservation treatment gels into paint films studied by unilateral NMR: Part I: Acrylic emulsion paint, Microchem. J. 124 (2016) 311–320.
[35] K. Ulrich, S.A. Centeno, J. Arslanoglu, E. Del Federico, Absorption and diffusion measurements of water in acrylic paint films by single-sided NMR, Prog. Org. Coat. 71 (3) (2011) 283–289.
[36] V. Di Tullio, G. Sciutto, N. Proietti, S. Prati, R. Mazzeo, C. Colombo, E. Cantisani, V. Romè, D. Rigaglia, D. Capitani, ^{1}H NMR depth profiles combined with portable and micro-analytical techniques for evaluating cleaning methods and identifying original, non-original, and degraded materials of a 16th century Italian wall painting, Microchem. J. 141 (2018) 40–50.
[37] G.R. Fife, B. Stabik, A.E. Kelley, J.N. King, B. Blümich, R. Hoppenbrouwers, T. Meldrum, Characterization of aging and solvent treatments of painted surfaces using single-sided NMR, Magn Reson Chem. 53 (1) (2015) 58–63.
[38] V. Di Tullio, N. Zumbulyadis, S.A. Centeno, J. Catalano, M. Wagner, C. Dybowski, Water Diffusion and Transport in Oil Paints as Studied by Unilateral NMR and 1H High-Resolution MAS-NMR Spectroscopy, ChemPhysChem 21 (1) (2020) 113–119.
[39] G. Lipari, A. Szabo, Model-free approach to the interpretation of nuclear magnetic resonance relaxation in macromolecules. 1. Theory and range of validity, J. Am. Chem. Soc. 104 (1982) 4546–4559.
[40] P. Berman, O. Levi, Y. Parmet, M. Saunders, Z. Wiesman, Laplace inversion of low-resolution NMR relaxometry data using sparse representation methods, *Concepts Magn*, Reson. A: Bridg. Educ. Res. 42 (3) (2013) 72–88.
[41] E.J. Fordham, What are, and what nare not, Inverse Laplace Trasformation, Diffusion Fundamentals, 2017.
[42] S.W. Provencher, Inverse problems in polymer characterization: Direct analysis of polydispersity with photon correlation spectroscopy, Makromol. Chem. 180 (1979) 201–211.
[43] G.C. Borgia, R.J.S. Brown, P. Fantazzini, Uniform-penalty inversion of multiexponential decay data, J. Magn. Reson. 1321 (1998) 65–77.
[44] C.A. Sholl, A BPP (Bloembergen-Purcell-Pound) model for nuclear spin relaxation due to diffusion in disordered systems: combined barrier- and site-energy disorder, J. Phys.: Condens. Matter. 12 (2000) 4285.
[45] S.F. Edwards, The theory of polymer solutions at intermediate concentration, Proc. Phys. Soc. 88 (1966) 265–280.
[46] P.G. De Gennes, Dynamics of Entangled Polymer Solutions. I. The Rouse Model, Macromolecules 9 (1976) 587–593.
[47] L. Baij, J.J. Hermans, K. Keune, P.D. Iedema, Time-Dependent ATR-FTIR Spectroscopic Studies on Solvent Diffusion and Film Swelling in Oil Paint Model Systems, Macromolecules 51 (18) (2018) 7134–7144.
[48] L. Brannon-Peppas, R.S. Harland, The Equilibrium Swelling Behavior of Porous and Non-Porous Hydrogels, Prog. Polym. Sci. 8 (1990) 67–102.
[49] S. Iqbal, F. Rodríguez-LLansola, B. Escuder, J.F. Miravet, I. Verbruggenb, R. Willem, HRMAS 1H NMR as a tool for the study of supramolecular gels, Soft Matter 6 (2010) 1875–1878.

[50] Alam, T. M.; Jenkins, J.E. HR-MAS NMR Spectroscopy in Material Science, in Advanced Aspects of Spectroscopy, Muhammad Akhyar Farrukh (Ed.), ISBN: 978-953-51-0715-6, InTech, 2012.

[51] C. Kehlet, F. Kuvvetli, A. Catalano, J. Dittmer, Solid-state NMR for the study of Asger Jorn's paintings, Microchem. J 125 (2016) 308–314.

[52] van Krevelen, D.M.,Nijenuis, KE, Propreties of Polymers, Elsevier Ed., 2009.